

# Constraining $^{26}\text{Al}+p$ resonances using $^{26}\text{Al}(^3\text{He},d)^{27}\text{Si}$

R. B. Vogelaar,\* L. W. Mitchell,† and R. W. Kavanagh

*W. K. Kellogg Radiation Laboratory, California Institute of Technology, Pasadena, California 91125*

A. E. Champagne‡

*Department of Physics, Princeton University, Princeton, New Jersey 08544*

P. V. Magnus,§ M. S. Smith,|| A. J. Howard, and P. D. Parker

*A. W. Wright Nuclear Structure Laboratory, Yale University, New Haven, Connecticut 06511*

H. A. O'Brien

*Los Alamos National Laboratory, Los Alamos, New Mexico 87545*

(Received 1 November 1995)

The  $^{26}\text{Al}(^3\text{He},d)^{27}\text{Si}$  reaction was measured from  $0^\circ \leq \theta_{\text{c.m.}} \leq 35^\circ$  at  $E(^3\text{He})=20$  MeV using a quadrupole-dipole-dipole magnetic spectrometer. States in  $^{27}\text{Si}$  were observed above the background at 7652 and 7741 keV and upper limits were set for the state at 7592 keV. Implications for the  $^{26}\text{Al}(p,\gamma)^{27}\text{Si}$  stellar reaction rate are discussed.

PACS number(s): 25.55.Hp, 26.20.+f, 27.30.+t

## I. INTRODUCTION

Interest in the origin of  $^{26}\text{Al}$  following observation of its decay radiation in the galactic plane [1–6] and its isotopic residues in meteorites [7,8] has prompted measurements of the reactions involved in its production and destruction. Prior to the present work, resonances in the  $^{26}\text{Al}(p,\gamma)^{27}\text{Si}$  destruction reaction as low as  $E_p=288$  keV had been observed directly [9]. Spectroscopy of transfer reactions on stable targets by Wang *et al.* [10] and others [11] has revealed seven states in  $^{27}\text{Si}$  at lower energies (Fig. 1). Some of the proposed  $^{26}\text{Al}$  production sites involve temperatures below  $10^8$  K ( $T_9=0.1$ ) at which one of these lower states could dominate the reaction rate. Since the  $J^\pi=5^+$  ground state of  $^{26}\text{Al}$  strongly favors formation of high-spin states in  $^{27}\text{Si}$ , the spins (as well as spectroscopic strengths) of the observed states are needed. Because Wang *et al.* [10] could not extract this information directly from their data, they identified low-spin states in the analogous region in  $^{27}\text{Al}$  in an effort to eliminate from further consideration states in  $^{27}\text{Si}$  which could not correspond to astrophysically interesting resonances.

To avoid this dependence on uncertain analog assignments, we developed a thin target of radioactive  $^{26}\text{Al}$  to ex-

amine the  $^{26}\text{Al}(^3\text{He},d)^{27}\text{Si}$  reaction. This reaction is expected to proceed by direct proton transfer in which the angular distribution of the outgoing deuteron reflects the  $l$  transfers involved, and the flux of each deuteron group is proportional to the proton width,  $\Gamma_p$ , of the residual state. The thermonuclear reaction rate for an isolated narrow resonance at  $E_r$  is given in the center-of-mass system by

$$\langle \sigma v \rangle = \left( \frac{2\pi}{\mu kT} \right)^{3/2} \hbar^2 (\omega \gamma) \exp\left( \frac{-E_r}{kT} \right).$$

The quantity  $\mu$  is the reduced mass and  $\omega \gamma$  is the resonance strength, which is defined by

$$\omega \gamma = \frac{2J+1}{(2J_t+1)(2J_p+1)} \frac{\Gamma_p \Gamma_\gamma}{\Gamma}.$$

Here,  $J$ ,  $J_t$ , and  $J_p$  refer to the spins of the final state, target, and incident proton, respectively, and  $\Gamma_p$ ,  $\Gamma_\gamma$ , and  $\Gamma$  are the proton and  $\gamma$ -ray partial widths, and the total width, respectively. Since the energies of interest are sufficiently low that the Coulomb barrier makes the proton width much less than the  $\gamma$ -ray width,  $\omega \gamma \approx (2J+1)\Gamma_p/22$  for the  $^{26}\text{Al}(p,\gamma)^{27}\text{Si}$  reaction. The proton width may be obtained from the familiar relation  $\Gamma_p = C^2 S \Gamma_{\text{s.p.}}$  where  $C^2 S$  is the proton spectroscopic factor measured via the  $(^3\text{He},d)$  reaction, and  $\Gamma_{\text{s.p.}}$  is the single-particle width. The results of the present  $^{26}\text{Al}(^3\text{He},d)^{27}\text{Si}$  work indicated the probable existence of an  $^{26}\text{Al}(p,\gamma)^{27}\text{Si}$  resonance near  $E_p=195$  keV, and prompted a subsequent sensitive search [13] which succeeded in directly measuring its energy and strength (see Sec. V).

## II. TARGET

The production and purification of the  $^{26}\text{Al}$  target material is described elsewhere [13,14]. A transmission target on a thin carbon foil was made by evaporation of  $\text{Al}_2\text{O}_3$  ( $^{26}\text{Al}/^{27}\text{Al}=6.3 \pm 0.1\%$ ) from a graphite boat brought to 2475

\*Present address: Physics Department, Princeton University, Princeton, NJ 08544.

†Present address: Department of Physics, Flinders University, Bedford Park 5042, Australia.

‡Permanent address: Department of Physics and Astronomy, University of North Carolina at Chapel Hill, Chapel Hill, NC 27599 and Triangle Universities Nuclear Laboratory, Duke University, Durham, NC 27706.

§Present address: Department of Physics, University of Washington, Seattle, WA 98195.

||Present address: Oak Ridge National Laboratory, Oak Ridge, TN 37831.

$E_x$ ( $^{27}\text{Si}$ )	$E_p$	
7893	446	
7831	381	
7792	341	
7741	288	
7702	247	
7652	195	
7592	133	
7557	97	
7532	71	
7468	4	$\frac{^{26}\text{Al} + p}{7464}$
7436		

FIG. 1. Excitation energies in  $^{27}\text{Si}$  near the  $^{26}\text{Al}+p$  threshold and their corresponding resonance energies in  $^{26}\text{Al}(p,\gamma)^{27}\text{Si}$ . Energies are in keV [12].

K for 15 sec six times, allowing a cooling period between each heating. Attempts using premounted self-supporting carbon foil backings failed owing to poor adhesion of the  $\text{Al}_2\text{O}_3$ , whereas successful targets were obtained by first evaporating a  $40 \mu\text{g}/\text{cm}^2$  carbon film directly onto a lightly etched  $76 \mu\text{m}$  Cu foil which was itself clamped to a larger Cu heat sink. After the  $\text{Al}_2\text{O}_3$  was deposited, a  $10 \mu\text{g}/\text{cm}^2$  overlay of carbon was then added in order to further stabilize the target against mechanical or other loss mechanisms.

The four-layer foil (Cu, C,  $\text{Al}_2\text{O}_3$ , C) was laid, carbon face down, over a tantalum frame coated with a thin film of vacuum grease and having a 6.4 mm diameter centered hole. The excess foil was folded over the edges of the frame for support. An etching solution (1 ml  $\text{H}_2\text{O}$ :1.1 ml 13M  $\text{NH}_4\text{OH}$ :1 g trichloroacetic acid) was made to flow gently over the Cu side of the target to remove the copper foil.

The energy resolution of the deuteron group to be searched for is determined by beam-energy resolution, detector resolution, energy straggling in the target, and, for forward-angle detection, the difference in energy loss between  $^3\text{He}$  and deuterons passing through the target. The known level density in  $^{27}\text{Si}$  necessitated a resolution of  $\leq 15$  keV which placed an upper limit on the target thickness. The final target was analyzed using Rutherford backscattering (Fig. 2), and by integrating the yield of the 992 keV resonance in  $^{27}\text{Al}(p,\gamma)^{28}\text{Si}$ . The total surface density was  $\approx 55 \mu\text{g}/\text{cm}^2$ , with  $(0.60 \pm 0.03) \mu\text{g}/\text{cm}^2$  of  $^{26}\text{Al}$  and the observed

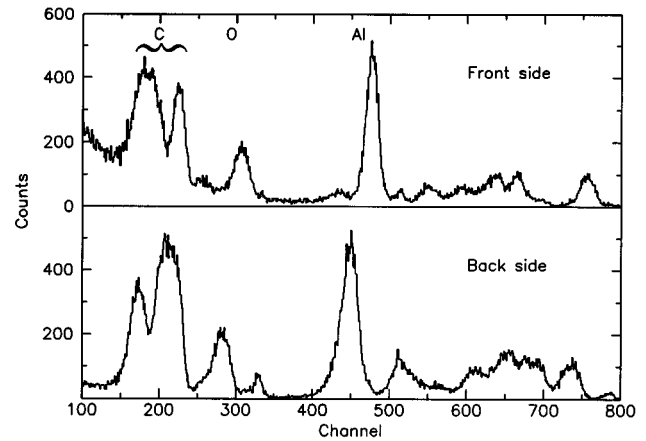


FIG. 2. Rutherford backscattering of 2 MeV  $\alpha$  particles. The double carbon peak reflects the target's layered structures. Reversing the target shifts the Al and O peaks by the difference in thickness of the two carbon films. Other structure comes from target contaminants and pin holes in the carbon.

resolution was  $\approx 12$  keV. A reference target of natural Al ( $^{27}\text{Al}$ ) was made in an identical fashion.

### III. EXPERIMENTAL PROCEDURE

A 20 MeV  $^3\text{He}$  beam was supplied by the Princeton AVF cyclotron, and the outgoing deuterons were analyzed using a dispersion-matched quadrupole-dipole-dipole-dipole (QDDD) magnetic spectrometer. The focal-plane detector consisted of a position-sensitive gas proportional counter ( $\Delta E$ ), followed by a plastic scintillator ( $E-\Delta E$ ) that allowed for standard particle identification.

The momentum bite afforded by the 60-cm-long focal-plane detector allowed us to study deuteron groups corresponding to population of states in  $^{27}\text{Si}$  between about 7.25 and 8.25 MeV excitation. Deuteron-energy calibration and absolute yields were determined from known particle groups arising from  $^{27}\text{Al}(^3\text{He},d)^{28}\text{Si}$  reactions on the  $^{27}\text{Al}$  in the tar-

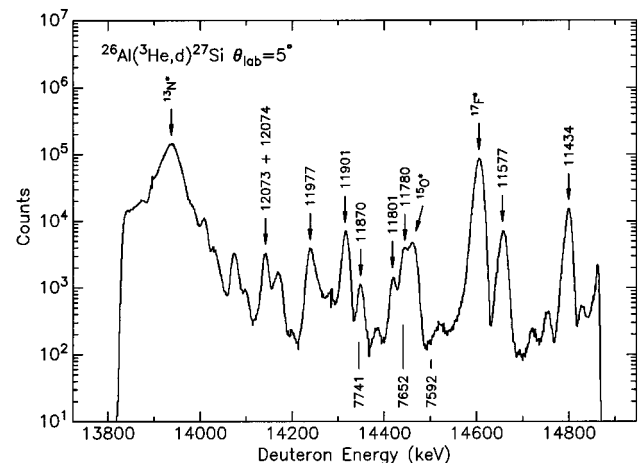


FIG. 3. Deuteron groups identified by the excited state of the residual nucleus. Those from  $^{28}\text{Si}$  are labeled above the curve, while those from  $^{27}\text{Si}$  states are labeled below.

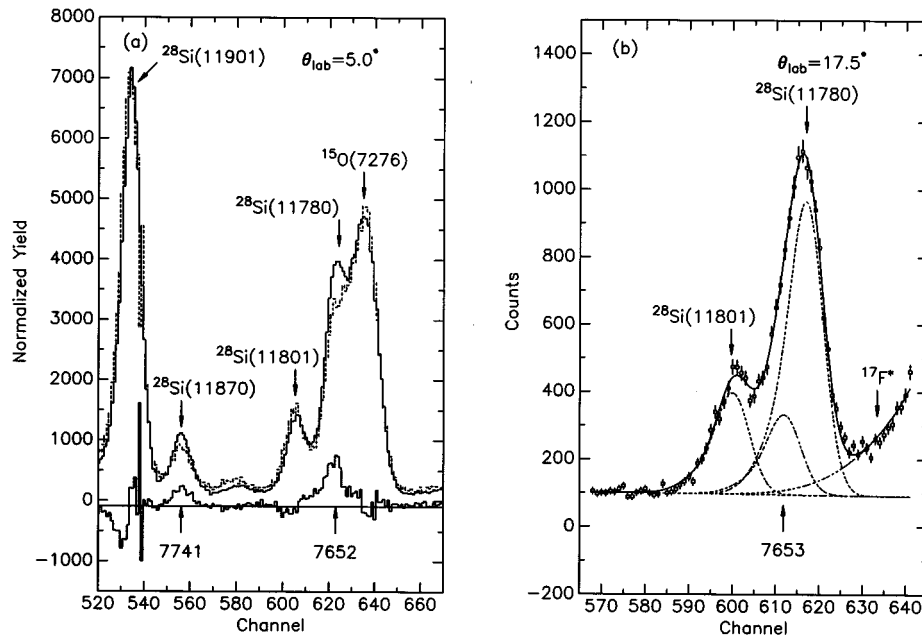


FIG. 4. Examples of (a) subtraction and (b) fitting analyses described in the text. In (a) the dashed line corresponds to the  $^{27}\text{Al}$  calibration target while the upper solid line corresponds to the 6.3%  $^{26}\text{Al}$  target; the low solid line corresponds to the net  $^{26}\text{Al}(^3\text{He},d)^{27}\text{Si}$  yield after subtraction. Notice the difference in line shape between the Si and F groups in the  $17.5^\circ$  spectrum. Residual groups attributed to  $^{27}\text{Si}$  are labeled below the curves.

get [15]. Data were collected at  $\theta_{\text{lab}}=0, 5, 10, 13, 15, 17.5, 20, 30,$  and  $35$  deg.

#### IV. ANALYSES

A representative deuteron spectrum at  $\theta_{\text{lab}}=5^\circ$  is presented in Fig. 3. The spectrum is clearly dominated by products of the  $^{27}\text{Al}(^3\text{He},d)^{28}\text{Si}$  reaction, as well as by deuterons arising from reactions on  $^{12}\text{C}$ ,  $^{16}\text{O}$ , and  $^{14}\text{N}$  (the  $^{14}\text{N}$  perhaps coming from ammonia in the copper etch). Spectra taken with the reference  $^{27}\text{Al}$  target were gain matched and normalized (using strong, isolated peaks arising from  $^{27}\text{Al}$ ) to those of the  $^{26}\text{Al}$  target, and then subtracted from the  $^{26}\text{Al}$  spectra. Two residual peaks were observed and their kinematic energy change with angle was consistent with production arising from the  $A=26$  component of the target. An energy calibration, based upon the well-known states in  $^{28}\text{Si}$  indicated that these peaks corresponded to the 7652 and 7741 keV states in  $^{27}\text{Si}$ . Additionally, at several angles the region of interest for the 7592 keV state was clear of background, so an upper limit on its strength could be established. Absolute cross sections were then obtained from the  $^{26}\text{Al}/^{27}\text{Al}$  ratio and the known  $^{27}\text{Al}(^3\text{He},d)^{28}\text{Si}$  cross sections [15]. Because of the large background elsewhere, no information was obtained for other states in  $^{27}\text{Si}$ .

This straightforward approach assumed that contributions from contaminants were the same for each target and that the line shapes did not vary between runs. To avoid relying entirely upon these assumptions, we developed a fitting procedure in which isolated deuteron groups from  $^{28}\text{Si}$  states were used to define a single ‘‘Si’’ line shape for each spectrum and yields from  $^{28}\text{Si}$  states were held to their known relative strengths [15]. Other contaminant line shapes were taken from fits to the reference target data, and the ratio of the

yields obtained with the two targets was indeed constant for all angles. Remaining parameters, viz., a linear background, centroids, and independent amplitudes, were then varied to minimize  $\chi^2$ . The fits included the nearest two or three peaks to the one of interest (Fig. 4).

The particle-group centroids returned by this procedure are presented in Fig. 5. Centroids of the 11780 and 11901 keV  $^{28}\text{Si}$  groups were used as calibration points, and then the difference of each centroid from that of the 11901 keV level was plotted against exit angle. The curves shown were calculated using known kinematic relations and level spacings. The background  $^{15}\text{O}$  group, whose line shape changed drastically with angle, appears to have been handled successfully based on the kinematic shift of its centroid. More signifi-

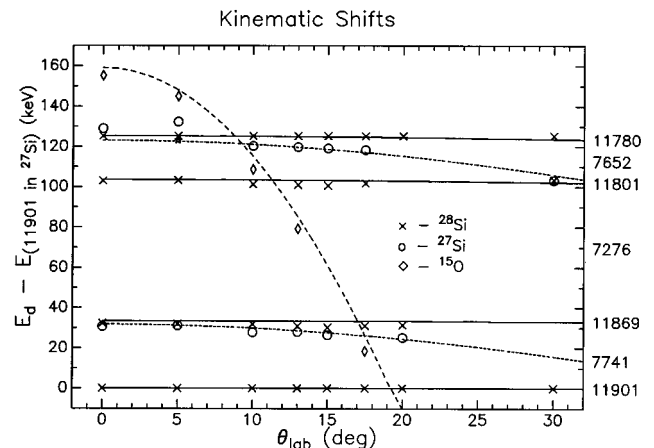


FIG. 5. Expected kinematic shifts of deuteron groups are shown by smooth curves. Actual observations are indicated and confirm that the 7741- and 7652-keV groups come from a mass 26 target.

TABLE I. DWBA parameters [15,19].

Channel	$V$ (MeV)	$r$ (fm)	$a$ (fm)	$W$ (MeV)	$W'$ (MeV)	$r'$ (fm)	$a'$ (fm)	$V_{SO}$ (MeV)	$r_c$ (fm)
$^{26}\text{Al}+^3\text{He}$	159	1.15	0.68	17.86		1.57	0.88		1.25
$^{27}\text{Si}+d$	39	1.30	0.88		89	1.48	0.54		1.30
$^{26}\text{Al}+p$	varied <sup>a</sup>	1.25	0.65					$\lambda=25$	1.25

<sup>a</sup>Adjusted to give the correct resonance energy.

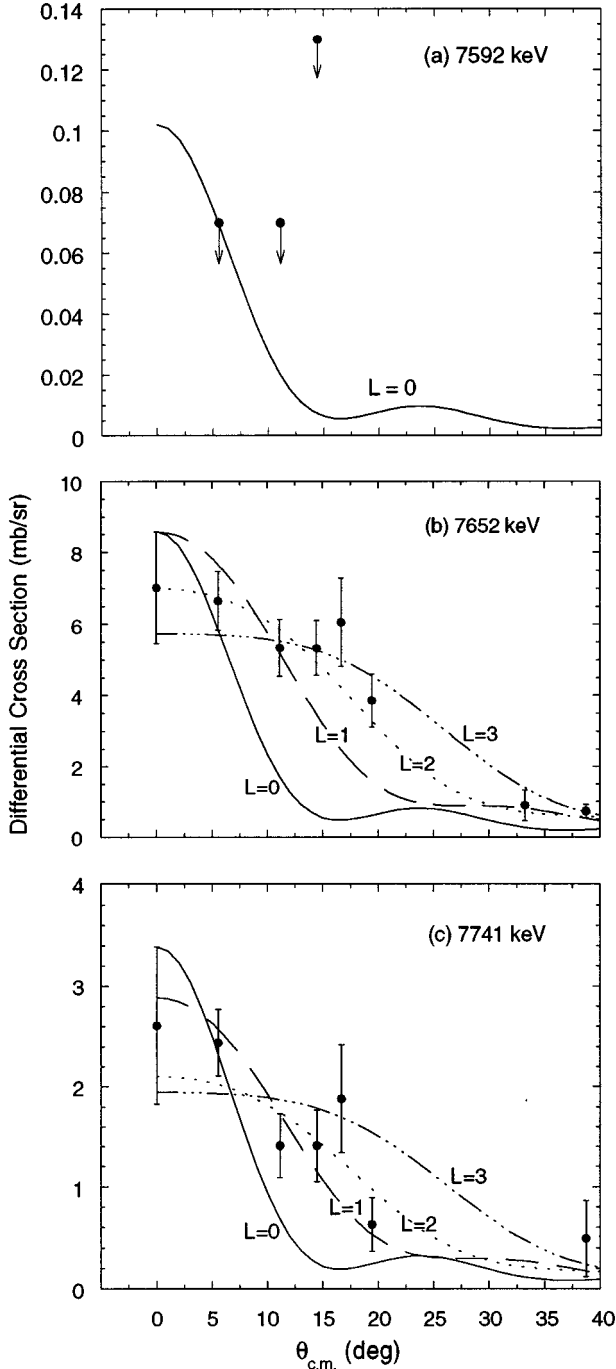


FIG. 6. Angular distributions and DWBA fits for the states of interest.

cantly, the two peaks of interest are again consistent with an  $A=26$  target. At some angles fitting became impractical because of background peaks that moved into the fit region.

The yields of the  $^{27}\text{Si}$  groups obtained by this fitting procedure were consistent with those obtained by direct subtraction, and the two sets of results were combined by taking weighted averages for the cross sections and errors using the method of Wohl *et al.* [16]. Spectroscopic factors were obtained from the relationship between the measured cross section,  $d\sigma/d\Omega(\text{expt})$ , and that calculated using the distorted-wave Born approximation (DWBA) code DWUCK4 [17]:

$$\frac{d\sigma}{d\Omega}(\text{expt}) = N C^2 S \left( \frac{2J+1}{(2J_i+1)(2J_f+1)} \right) \frac{d\sigma}{d\Omega}(\text{DWBA}),$$

where  $N$  is an overall normalization (equal to 4.42 for this reaction [18]);  $C^2 S$  is the aforementioned spectroscopic factor; and  $J_i$  and  $J$  are the spins of the target and final state, respectively, while  $J_i$  is the transferred angular momentum. Optical-model parameters appropriate for this mass and energy region were used [19] (summarized in Table I) and the transferred proton was treated using an unbound form factor. Since  $J_i$  is not uniquely determined by  $l$ , we have chosen  $2s_{1/2}$ ,  $2p_{3/2}$ ,  $1d_{3/2}$ , and  $1f_{7/2}$  transfers. The uncertainty resulting from this ambiguity in the angular-momentum transfer is small compared to the other uncertainties that enter in  $\omega\gamma$ . The angular distributions (shown in Fig. 6) are not particularly distinctive, and the nonzero spin of the target allows for the possibility of mixed  $l$  transfers. Consequently, we were not able to deduce unique  $l$  assignments. The spectroscopic factors shown in Table II were obtained under various assumptions for pure  $l$  transfers, and this represents the largest source of uncertainty in  $\omega\gamma$ . Single-particle widths were then

TABLE II. Spectroscopic factors and resonance strengths.

$E_p$ (keV)	$E_x(^{27}\text{Si})$ (keV)	$l$	$(2J+1)C^2 S^a$	$\omega\gamma$ (meV)	$\omega\gamma(\text{lit})^b$ (meV)
133	7592	0	<0.02	$<5.9 \times 10^{-6}$	$<5.7 \times 10^{-3}$
195	7652	0	2.1	0.29	<0.042
		1	1.9	0.064	0.055 <sup>c</sup>
		2	4.2	$<3.2 \times 10^{-3}$	
		3	5.9	$<9.9 \times 10^{-5}$	
288	7741	0	0.87	19.0	2.9 <sup>c</sup>
		1	0.64	3.60	
		2	1.24	0.17	
		3	1.99	$<7.0 \times 10^{-3}$	

<sup>a</sup>Assuming  $2s_{1/2}$ ,  $2p_{3/2}$ ,  $1d_{3/2}$ , and  $1f_{7/2}$  transfer.

<sup>b</sup>Reference [10] unless noted.

<sup>c</sup>Reference [13].

calculated using the same form factors employed in the DWBA calculations. The resulting resonance strengths for pure  $l$  transfers are also listed in Table II.

## V. CONCLUSIONS

Our upper limit for the resonance strength corresponding to the 7592 keV state in  $^{27}\text{Si}$  is at least 200 times weaker than the limit obtained by Wang *et al.* [10] under the assumption that this was a pure single-particle state. On the other hand, the 7652 keV state is found to be a strong single-particle state and with a maximum  $l$  transfer of 3 (estimated from Fig. 6), it increases the experimental limit on  $\langle\sigma v\rangle$  at  $T_9\approx 0.1$  by more than two orders of magnitude. This measurement exemplifies the general role of spectroscopic studies in identifying states that warrant further study through direct observation of the reaction in question, where complete excitation functions are frequently impossible because of the low rates involved. In this case, the large spectroscopic factors found here for the 7652 keV state prompted further direct  $(p, \gamma)$  measurements described elsewhere [13] which

did, in fact, observe a resonance at 195 keV in  $^{26}\text{Al}(p, \gamma)^{27}\text{Si}$  having  $\omega\gamma=55\pm 9 \mu\text{eV}$ . The 7741 keV state is also a strong single-particle state. In this case,  $(p, \gamma)$  measurements had already been performed [9,13] and the measured resonance strength falls within the range listed in Table II.

Since we were not able to observe any states below  $E_p=195$  keV in the  $^{26}\text{Al}+p$  system, there are sizable uncertainties in the reaction rate for  $T_9<0.1$ . Although the 7592 keV state was too weak to be observed in the present measurement, our upper limit on  $\omega\gamma$  is still sufficient for it to be astrophysically important: A recent theoretical study [20] reported a resonance strength similar to our limit, with a major contribution to the reaction rate at low temperatures. Further information on the low-energy states will require a target with a significantly higher  $^{26}\text{Al}$  enrichment.

## ACKNOWLEDGMENTS

This work was supported in part by National Science Foundation Grant No. PHY88-17296 and in part by the U.S. Department of Energy.

- 
- [1] W. A. Mahoney, J. C. Ling, W. A. Wheaton, and A. S. Jacobson, *Astrophys. J.* **286**, 578 (1984).
  - [2] G. H. Share, R. L. Kinzer, J. D. Kurfess, E. L. Chupp, and E. Rieger, *Astrophys. J.* **292**, L61 (1985).
  - [3] C. J. MacCallum, A. F. Hutters, P. D. Stang, and M. Leventhal, *Astrophys. J.* **317**, 877 (1987).
  - [4] P. von Ballmoos, R. Diehl, and V. Schönfelder, *Astrophys. J.* **318**, 654 (1987).
  - [5] R. Diehl, C. Dupraz, K. Bennett, H. Bloemen, H. de Boer, W. Hermsen, G. G. Lichti, M. McConnell, D. Morris, J. Ryan, V. Schönfelder, H. Steinle, A. W. Strong, B. N. Swanenburg, M. Varendorff, and C. Winkler, *Astrophys. J. Suppl.* **92**, 429 (1994).
  - [6] R. Diehl, K. Bennett, H. Bloemen, C. Dupraz, W. Hermsen, J. Knödlseher, G. G. Lichti, D. Morris, U. Oberlack, J. Ryan, V. Schönfelder, H. Steinle, M. Varendorf, and C. Winkler, *Astron. Astrophys.* **298**, L25 (1995).
  - [7] T. Lee, D. A. Papanastassiou, and G. J. Wasserburg, *Astrophys. J.* **211**, L107 (1977).
  - [8] P. Hoppe, S. Amari, E. Zinner, T. Ireland, and R. S. Lewis, *Astrophys. J.* **430**, 870 (1994).
  - [9] L. Buchmann, M. Hilgemeier, A. Krauss, A. Redder, C. Rolfs, and H. P. Trautvetter, *Nucl. Phys.* **A415**, 93 (1994).
  - [10] T. F. Wang, A. E. Champagne, J. D. Hadden, P. V. Magnus, M. S. Smith, A. J. Howard, and P. D. Parker, *Nucl. Phys.* **A499**, 546 (1989).
  - [11] P. Schmalbrock, T. R. Donoghue, M. Wiescher, V. Wijekumar, C. P. Browne, A. A. Rollefson, C. Rolfs, and A. Vliks, *Nucl. Phys.* **A457**, 182 (1986).
  - [12] P. M. Endt, *Nucl. Phys.* **A521**, 1 (1990).
  - [13] R. B. Vogelaar, Ph.D. thesis, California Institute of Technology, 1989.
  - [14] K. W. Thomas, *Radiochim. Acta* **33**, 213 (1983).
  - [15] A. E. Champagne, M. L. Pitt, P. H. Zhang, L. L. Lee, Jr., and M. J. LeVine, *Nucl. Phys.* **A259**, 239 (1986).
  - [16] C. G. Wohl *et al.*, *Rev. Mod. Phys.* **56**, S1 (1984).
  - [17] P. D. Kunz, University of Colorado report, 1974 (unpublished); program DWUCK4, P.D. Kunz (unpublished); extended version of J. R. Comfort (unpublished).
  - [18] R. H. Bassel, *Phys. Rev.* **149**, 791 (1966).
  - [19] C. M. Perey and F. G. Perey, *At. Data Nucl. Data Tables* **17**, 1 (1976).
  - [20] A. E. Champagne, B. A. Brown, and R. Sherr, *Nucl. Phys.* **A556**, 123 (1994).